PHYSICAL REVIEW B **96**, 041303(R) (2017)

Determining the nature of excitonic dephasing in high-quality GaN/AlGaN quantum wells through time-resolved and spectrally resolved four-wave mixing spectroscopy

M. Gallart,[1,*] M. Ziegler,[1] O. Crégut,[1] E. Feltin,[2] J.-F. Carlin,[2] R. Butté,[2] N. Grandjean,[2] B. Hönerlage,[1] and P. Gilliot[1]

[1]*IPCMS UMR 7504 CNRS - Université de Strasbourg, 23 rue du Læss, BP 43, F-67034 Strasbourg Cedex 2, France*

[2]*Institute of Physics, Ecole Polytechnique Fédérale de Lausanne (EPFL), CH-1015 Lausanne, Switzerland*

(Received 26 April 2017; published 24 July 2017)

Applying four-wave mixing spectroscopy to a high-quality GaN/AlGaN single quantum well, we report on the experimental determination of excitonic dephasing times at different temperatures and exciton densities in III-nitride heterostructures. By comparing the evolution with the temperature of the dephasing and the spin-relaxation rate, we conclude that both processes are related to the rate of excitonic collisions. When spin relaxation occurs in the motional-narrowing regime, it remains constant over a large temperature range as the spin-precession frequency increases linearly with temperature, hence compensating for the observed decrease in the dephasing time. From those measurements, a value of the electron-hole exchange interaction strength of 0.45 meV at $T = 10$ K is inferred.

DOI: 10.1103/PhysRevB.96.041303

I. INTRODUCTION AND CONTEXT

Four-wave mixing (FWM) spectroscopy is an extremely powerful nonlinear optical pump-probe spectroscopy technique giving access to the decay of the time-integrated diffracted signal with increasing delay between the exciting pulses. In semiconductors, such decay provides a direct measure of the excitonic phase coherence, and the resulting characteristic decay time of the FWM intensity is the so-called dephasing or coherence time T_2. It is connected to the homogeneous linewidth broadening γ (also called the dephasing rate) by the relationship $T_2 = 2\hbar\gamma^{-1}$ [1].

The FWM technique has been applied to a wide range of material systems, including bulk GaAs and GaAs/AlGaAs quantum wells (QWs), where excitonic coherence was shown to be mainly determined by excitonic collisions. As an illustration, the influence of exciton- and free-carrier density, their interaction with phonons via a temperature increase, and the role of exciton localization were all explored. For three-dimensional (3D) and two-dimensional (2D) excitons, the dephasing time was found to lie in the picosecond range in this material family [2,3], whereas an ultralong dephasing time of several hundred picoseconds was reported in InGaAs/GaAs quantum dots [4] showing that wave-vector relaxation due to collisions is the dominant dephasing mechanism. It was also used to determine the binding energy of biexcitons in ultrahigh-quality GaAs/AlGaAs QWs [5]. The nonlinear optical properties of C_{60} were also accessed using this technique [6], and, more recently, FWM spectroscopy has been successfully used to probe the population and coherence dynamics of excitonic transitions in monolayers of transition-metal dichalcogenides [7]. In III nitrides, some pioneering works [8,9] focused on the optical coherence of excitons in GaN epilayers, but, to date, despite their technological importance for optoelectronics and high-power high-frequency electronics, data concerning III-nitride quantum heterostructures are lacking, even though such information would prove extremely useful to understand the spin physics of excitons in these systems.

Indeed, regardless of the spin-relaxation process at play, it always involves a relaxation of the wave vector. It is usually accepted that the spin relaxation of the exciton as a whole is the main cause of its spin relaxation in QWs [10]. It originates from a long-range electron-hole exchange interaction that is enhanced by quantum confinement along the growth direction. At finite wave vector $\mathbf{K}$, the spin-exchange interaction couples the optically active $|+1\rangle$ and $|-1\rangle$ excitons. The coupling terms in the Hamiltonian act as an effective magnetic field about which the exciton pseudospin precesses with a frequency Ω. If $\mathbf{K}$ is kept fixed, the direction of the effective magnetic field remains constant while the precession leads to spin relaxation when a scattering event occurs that modifies the direction of the $\mathbf{K}$ vector. Eventually, two limiting cases can be considered, depending on the ratio between the collision time τ_C of the excitons and the inverse of the precession frequency Ω: If $\tau_C > \Omega^{-1}$, the spin-relaxation time τ_S is proportional to the collision time τ_C, but, on the contrary, if $\tau_C < \Omega^{-1}$, the spin relaxation is hindered by motional narrowing and τ_S can be much longer than τ_C. As will be discussed hereafter, measuring the dephasing time T_2 of excitons will give valuable information on their collision time τ_C and thus on spin relaxation.

In this Rapid Communication, we report on the experimental determination of the excitonic dephasing time, measured at different temperatures and excitonic densities, in a high-quality GaN/AlGaN QW by means of FWM spectroscopy. We also provide a comparison of the evolution with temperature of both the dephasing- and the spin-relaxation rate.

II. SAMPLE AND EXPERIMENTAL SETUP

The studied sample is a high-quality low Al content single GaN/AlGaN QW grown by metal-organic vapor phase epitaxy on a c-plane sapphire substrate. The template is composed of a standard 3 μm thick GaN buffer layer and a 200 nm thick $Al_xGa_{1-x}N$ layer. A single GaN QW with a nominal thickness of 2.6 nm was then deposited and capped with a 50 nm thick $Al_xGa_{1-x}N$ layer with $x = 5\%$. More details on the structural and optical characterization of this sample can be

*Corresponding author: mathieu.gallart@ipcms.u-strasbg.fr

found in previous publications [11,12]. The overall quality of the resulting single GaN/AlGaN quantum well is very high, as shown by the small Stokes shift that is smaller than 4 meV [12].

The experimental setup is identical to the one employed in our previous population- and spin-dynamics measurements [13]. A homemade Ti:sapphire oscillator generates 80 fs pulses at a repetition rate of 82 MHz, which pass a regenerative amplifier, operating at 200 kHz, before being sent into an optical parametric amplifier, tuned close to 700 nm (1.770 eV). Pulses are frequency doubled with a β-BaB_2O_4 (BBO) crystal to reach the GaN exciton spectral region (3.50–3.55 eV). The pulse duration is estimated to be ∼200 fs. The pulse spectrum is broad (17 meV of full width at half maximum) and covers the entire spectral region that is related to active excitonic transitions in the QW. The FWM experiments are performed in a two-beam configuration. The spot size of the laser on the sample surface presents a typical diameter close to ∼100 μm. The coherent signal, measured as a function of the delay between the two exciting pulses, is collected in a backward configuration and analyzed by a spectrometer and a liquid-nitrogen-cooled CCD. Given the pulse duration, we evaluate the time resolution at ∼100 fs. The spectral resolution is 0.1 nm.

III. RESULTS

Figure 1 displays the intensity of the spectrally resolved FWM signal at low temperature ($T = 7$ K). The vertical scale is the time delay between two consecutive pulses while the horizontal scale is the photon energy. The feature at 3.48 eV is the coherent response of the GaN buffer layer whose time evolution is not resolved at this scale. Taking into account the strong absorption coefficient of GaN, we assume that the laser excitation essentially probes the superficial region of the buffer layer whose crystalline quality is affected in the vicinity of the interface with the first AlGaN barrier,

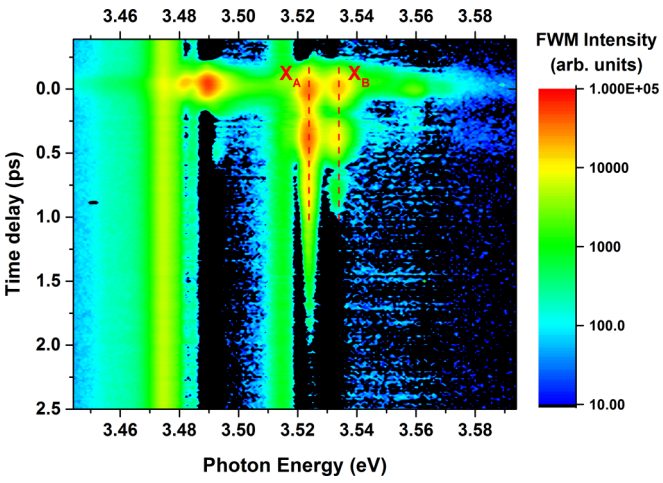

FIG. 1. Intensity of the time-resolved and spectrally resolved FWM signal of a GaN/$Al_{0.05}Ga_{0.95}N$ quantum well at low temperature ($T = 7$ K) at an average pump power equal to 0.8 W/cm^2. The vertical scale corresponds to the time delay between the pump-and-probe pulses while the horizontal scale displays the photon energy. X_A and X_B indicate the heavy- and light-hole exciton resonances, respectively.

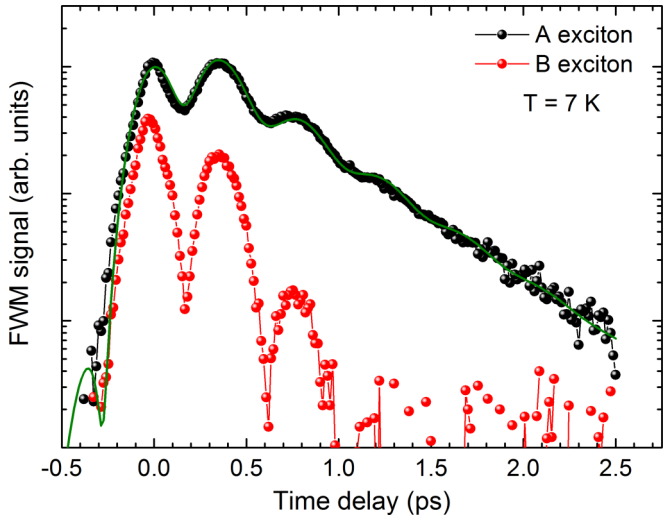

FIG. 2. Time profiles of the FWM signals for the A- (black line) and B-exciton (red line) resonances measured at their spectral maxima and plotted as a function of pulse delay. The green line is the best fit to the signal decay of the A exciton. The average pump power is 2 W/cm^2.

leading to very short dephasing times. Two resonances related to the QW excitons are centered at 3.526 and 3.536 eV, which are related to the A (heavy-hole) and B (light-hole) excitons, respectively. The time profiles of these signals at their spectral maxima are plotted in Fig. 2 as a function of pulse delay. They decay exponentially on a two-decade scale for both excitons and exhibit oscillations that do not present any phase shift as a function of detection wavelength and, therefore, originate from quantum beats between A and B excitons [14]. Moreover, the beat period (440 fs) is consistent with the 9.5 meV splitting measured between the heavy- and light-hole bands. A standard fitting procedure enables one to extract the decay time constants $\tau_{expt}(A) = 0.46$ ps and $\tau_{expt}(B) = 0.17$ ps for excitons A and B, respectively. At this stage, we need to determine the nature of the broadening to extract the numerical value of the dephasing time T_2 from the experimental decay time. As a matter of fact, in the case of pure homogeneous broadening, the FWM signal would decrease as $\exp(-2t/T_2)$, while for pure inhomogeneous broadening one would deal with a photon-echo signal that decays as $\exp(-4t/T_2)$. In the present sample, the hypothesis of pure homogeneous broadening cannot account, however, for the large broadening values extracted from linear reflectivity measurements, i.e., $\Gamma(A) = 5.9$ meV and $\Gamma(B) = 5.4$ meV [15]. We assume then that the main source of broadening is coming from inhomogeneities in the QW width and the AlGaN barrier composition. We conclude that the measured signal is a photon-echo signal and that the dephasing times of the two excitons are equal to $T_2(A) \approx 4\,\tau_{expt}(A) = 1.84$ ps and $T_2(B) \approx 4\,\tau_{expt}(B) = 0.68$ ps at low temperature, respectively.

In order to gain more information on the dephasing processes, the experiment was performed at different excitation powers and temperatures. Figure 3(a) displays the evolution of the homogeneous linewidths $\gamma(A)$ and $\gamma(B)$ (expressed in meV) of A and B excitons, calculated from $\tau_{expt}(A)$ and $\tau_{expt}(B)$, as a function of excitation power at $T = 27$ K.

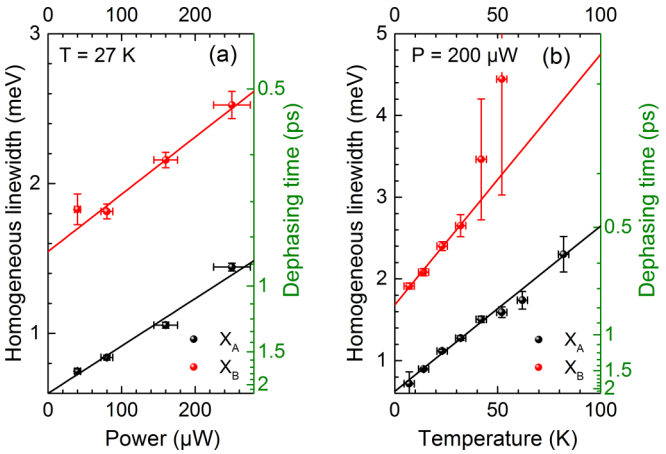

FIG. 3. Evolution of the measured dephasing rate of A and B excitons as a function of (a) pump power and (b) temperature. A shorter dephasing time and a weaker intensity result in a poor signal-to-noise ratio for the B exciton above 50 K, explaining the large error bars. The straight lines correspond to linear fits, as explained in the main text.

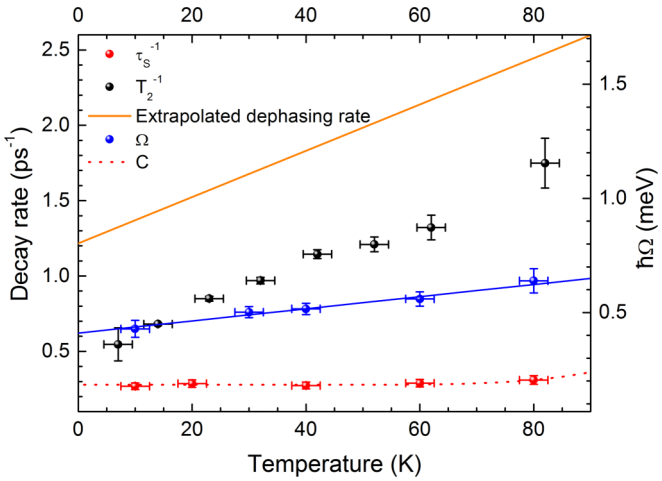

FIG. 4. Evolution of the dephasing rate T_2^{-1} (black circles) and of the spin-relaxation rate τ_S^{-1} (red circles from Ref. [13]) as a function of temperature. The dephasing rate is measured at an average excitation-power density of 20 W/cm^2 that corresponds, once focused onto the sample surface, to a finite density of incident photons of $\sim 1.8 \times 10^{13}$ cm^{-2} per pulse. The orange line is the variation of the dephasing rate T_2^{-1} that can be extrapolated from the data of Fig. 3(b) for the same density of excitons that was used to measure the spin-relaxation time τ_S. The electron-hole exchange interaction $\hbar\Omega$ (see text) that we calculate from those data are then plotted with blue circles.

Increasing the density of the photocreated excitons speeds up the dephasing due to exciton-exciton scattering. Thus, the dephasing rate shows a linear dependence on the excitation density, as usually observed in other QW systems [16].

A linear increase of the homogeneous linewidth with the sample temperature,

$$\gamma(T) = \gamma_0 + \beta T,$$

is observed, as demonstrated by the fits shown in Fig. 3(b). This behavior is the typical signature of an exciton interaction with acoustic phonons when the temperature is raised [3]. Longitudinal optical phonons do not play any role in this temperature range because their energy is as large as 92 meV in GaN. We obtain the values $\beta(A) = 20\,\mu$eV/K [$\beta(B) = 30\,\mu$eV/K] and $\gamma_0(A) = 0.62$ meV [$\gamma_0(B) = 1.68$ meV] for the temperature range 7 K $< T <$ 80 K. Above 80 K, the decay times of the FWM signal become too short to be measured owing to the time resolution of our experimental setup. The slopes obtained by the fitting procedure are of the same order of magnitude as those measured in GaN epilayers ($\sim 16\,\mu$eV/K) [8] or in GaAs QWs ($\sim 10\,\mu$eV/K) [17].

A. Collision rate and motional-narrowing regime for spin relaxation

In a previous paper [13], we presented results on the spin-relaxation dynamics of excitons in the present single QW. Pump-probe experiments using circularly polarized pulses showed that the spin lifetime of excitons is close to 4 ps at low temperature (8 K). We have also shown that a long-range exchange interaction between the electron and the hole within the exciton is responsible for spin relaxation. Here, we aim at comparing the evolution with the temperature of both the spin lifetime τ_S and the dephasing time T_2 of excitons in order to gain more insight into the spin-relaxation process in GaN/AlGaN QWs. For this reason, Fig. 4 displays the measured spin decay rates τ_S^{-1} (taken from Ref. [13]) and T_2^{-1} of the A exciton as a function of temperature. As described above, in the 10–80 K range, the dephasing rate increases linearly while the spin-relaxation rate remains roughly constant. As indicated above, the latter will be mostly sensitive to inelastic exciton scattering events.

The exciton collision rate can be directly deduced from measurements of the dephasing rate T_2^{-1} through FWM experiments. Indeed, T_2^{-1} can be split into two contributions [1],

$$\frac{1}{T_2} = \frac{1}{2T_1} + \frac{1}{T_2^*}.$$

For the A exciton, the first contribution, related to the population recombination rate, is very small, as the lifetime T_1 lies within the hundreds of picosecond range [13]. Note that this is not the case for the B exciton where the transfer toward the A exciton states takes only a few ps [13]. The dephasing time T_2 of the A exciton is thus mainly determined by the pure dephasing time T_2^* that is due to collisions of the excitons with defects, phonons, and other excitons, $T_2^* = \tau_C$. Even at low exciton and phonon densities, for measurements performed at low excitation intensities and low temperatures, respectively, changes in the wave vector are the main source of dephasing.

The exciton-spin relaxation is caused by the electron-hole exchange interaction that lifts the degeneracy between optically active states with total angular momentum $|+1\rangle$ and $|-1\rangle$ when the center-of-mass wave vector $\mathbf{K}$ takes a finite value. This exchange-energy splitting $\hbar\Omega$ results in an exciton-spin precession at a frequency Ω about an effective magnetic field whose direction depends on $\mathbf{K}$. If the direction of $\mathbf{K}$ is randomly changed at a frequency higher than Ω, the time-averaged value of the effective magnetic field (seen by the

exciton) becomes null and spin relaxation is partially hindered. This situation is evidenced by experimental data shown in Fig. 4: Even if the exciton-phonon collisions follow the increase in the phonon population with temperature, as shown by the rise of the exciton dephasing rate T_2^{-1}, the spin lifetime τ_S (data of τ_S are taken from Ref. [13]) remains constant up to 80 K. It clearly evidences the motional narrowing of spin relaxation.

B. Spin-precession frequency and electron-hole exchange interaction

With the typical relaxation time of the wave vector being the dephasing time T_2, the relation between τ_S, T_2, and Ω is written in the motional-narrowing regime [10] as $\tau_S = (\Omega^2 T_2)^{-1}$.

For a constant precession frequency Ω, this should lead to an increase in the spin-relaxation time τ_S, resulting from the decrease in T_2 when the temperature is raised. This is obviously not the case, as shown by the measurements of Fig. 4. For small $\mathbf{K}$ values the precession frequency Ω is indeed known to be nearly proportional to the wave vector $\mathbf{K}$ [18]. When the temperature is increased, excitons statistically populate states with larger wave vectors, leading to an increase in the exchange interaction $\hbar\Omega(\mathbf{K})$. Considering a two-dimensional quantum well and averaging over the thermal $\mathbf{K}$ distribution of excitons with kinetic energy $E_c \propto K^2$, we can calculate the mean value of $\Omega^2(K)$,

$$\langle\Omega^2\rangle \propto \frac{\iint \Omega^2(K) e^{-\frac{E_C}{k_B T}} d^2K}{\iint e^{-\frac{E_C}{k_B T}} d^2K} \propto \frac{\iint K^2 e^{-\frac{K^2}{k_B T}} d^2K}{\iint e^{-\frac{K^2}{k_B T}} d^2K} \propto T.$$

It shows that a linear dependence of $\langle\Omega^2(K)\rangle$ with T is expected. This linear increase in the dephasing rate is exactly compensated by the linear decrease in the exchange interaction, resulting in a nearly constant spin lifetime, as experimentally observed.

By using our experimental values of τ_S and T_2, we can, moreover, give a numerical estimate of the precession frequency Ω and consequently of the exchange interaction strength. To perform this calculation we have extrapolated the dephasing rate $T_2^{-1}(A)$ in order to get its value under the same excitation conditions as those used to measure the spin dynamics: This is plotted as a continuous orange line in Fig. 4. This was possible owing to the data summarized in Fig. 3. We have then determined the experimental value of the precession frequency by using the equation $\Omega = (\tau_S T_2)^{-1/2}$. The result of this calculation is also shown in Fig. 4 (blue circles).

At low temperature (10 K), we find $\hbar\Omega \approx 0.45 \pm 0.1$ meV. This value is close to the value of 0.6 ± 0.1 meV measured at 2 K by Julier *et al.* in GaN epilayers grown on an *a*-plane sapphire [19]. This is additional evidence that the relation $\Omega = (\tau_S T_2)^{-1/2}$ is valid at least up to ∼80 K and that our interpretation about spin relaxation is correct. Because of the large exchange interaction, the precession-frequency variation $0.6\,\mathrm{ps}^{-1} < \Omega < 1\,\mathrm{ps}^{-1}$ is significant in the spanned temperature range. However, the large value of the dephasing rate and its linear evolution with temperature ensure a constant spin lifetime τ_S owing to motional narrowing. From a quantitative point of view, a comparison between our values and those of Ref. [19] does not show any clear enhancement of $\hbar\Omega$ when switching from epilayers to QWs.

The increase of the exchange interaction when going from 3D to 2D material was experimentally observed and modeled in GaAs/AlGaAs QWs [20]. Calculations showed that the enhancement factor is proportional to $(|\Phi_{\mathrm{QW}}(0)|/|\Phi_{\mathrm{3D}}(0)|)^2 \int_{-\infty}^{+\infty} |\psi_e(z_e)\psi_h(z_h)|^2 dz$, where $\psi_e(z_e)$ and $\psi_h(z_h)$ are the envelope functions of the electron and the hole along the growth axis, while $|\Phi_{\mathrm{QW}}(x,y,z)|$ and $|\Phi_{\mathrm{3D}}(x,y,z)|$ describe the electron-hole relative motion within the exciton in a QW and in the bulk, respectively. In a symmetric QW, the electron-hole overlap $\int_{-\infty}^{+\infty} |\psi_e(z_e)\psi_h(z_h)|^2 dz$ along the z axis is close to unity and does not vary significantly with increasing well width. The increase of the exchange interaction is mainly caused by the reduction of the exciton Bohr radius through the ratio $(|\Phi_{\mathrm{QW}}(0)|/|\Phi_{\mathrm{3D}}(0)|)^2$ by quantum confinement. Thus, the enhancement is expected to become substantial for well widths equal to or inferior to the bulk Bohr radius provided the barrier height is sufficient to confine the exciton inside the QW. In the present GaN/AlGaN QW, the latter conditions are not fulfilled: The well nominal width (2.6 nm) is close to the bulk GaN Bohr radius (≈2.8 nm) [21] and the low Al fraction in the confining barrier does not insure a satisfactory height [the energy difference between the *A* exciton in the QW and the barrier photoluminescence is ≈35 meV]. Moreover, we cannot exclude the influence of the built-in electric field, due to piezoelectric and spontaneous polarizations. In spite of the low Al composition in the barrier, the electric field has been estimated to be ∼270 kV/cm inside the QW in a previous work [22]. For III-nitride QWs, this value of the electric field can seem to be a rather moderate one as the electric field can reach several MV/cm for wide Al-rich cladding barriers. However, combined with a small barrier height, it enables a spatial separation of electrons and holes along the z axis as well as a decrease in the exchange interaction via the overlap integral $\int_{-\infty}^{+\infty} |\psi_e(z_e)\psi_h(z_h)|^2 dz$ [10]. Thus, we assume that, if an enhancement of the exchange interaction exists in our sample, it must be weak and the experimental uncertainties in both our work and Ref. [19] do not allow one to observe it.

IV. CONCLUSION

In the present Rapid Communication, we have investigated the evolution of the dephasing time of free excitons in a high-quality single GaN/AlGaN QW by means of spectrally resolved and time-resolved FWM as a function of temperature and excitation-power density.

Our results first deal with the coherence properties of the *A* and *B* excitonic transitions. Quantum beats with a period of 450 fs are measured, which are in good agreement with the splitting between the two exciton ground states. The low-density and low-temperature limits of the dephasing time T_2 as well as its evolution with increasing temperature and exciton density are fully characterized.

The measurement of the dephasing time T_2 allows one to determine the rate of collision τ_C^{-1} of excitons with phonons, within the exciton population, and with crystal defects. It provides valuable information about the mechanisms that

govern spin relaxation, where spin precession is expected between two interaction events. The spin-relaxation rate τ_S^{-1} remains constant for temperatures <80 K and is independent of the T_2 time. From a comparison with the dephasing rate T_2^{-1} we conclude that spin relaxation is affected by motional narrowing. We can even estimate the electron-hole exchange interaction that governs the exciton-spin precession to 0.45 meV at $T = 10$ K, with the frequency of the latter increasing with temperature.

Our results demonstrate that the combination of optical coherence decay measurements through FWM experiments and spin-relaxation measurements by polarized pump-and-probe experiments is very powerful in order to reveal the microscopic mechanisms that govern the spin dynamics in GaN-based heterostructures. The ability to perform such measurements at short wavelengths in a family of technologically mature semiconductors opens promising perspectives in view of fabricating advanced nanophotonic devices based on this platform. As an illustration, precise knowledge of the dephasing properties of nanoemitters would certainly prove extremely valuable, e.g., when embedding quantum dots in nanocavities exploiting cavity quantum electrodynamics phenomena such as the enhancement of the spontaneous emission rate via the Purcell effect.

[1] J. Shah, *Ultrafast Spectroscopy of Semiconductors and Semiconductor Nanostructures*, 2nd ed. (Springer, Berlin, 1999).

[2] L. Schultheis, J. Kuhl, A. Honold, and C. W. Tu, Phys. Rev. Lett. **57**, 1797 (1986).

[3] L. Schultheis, A. Honold, J. Kuhl, K. Köhler, and C. W. Tu, Phys. Rev. B **34**, 9027(R) (1986).

[4] P. Borri, W. Langbein, S. Schneider, U. Woggon, R. L. Sellin, D. Ouyang, and D. Bimberg, Phys. Rev. Lett. **87**, 157401 (2001).

[5] D. Birkedal, J. Singh, V. G. Lyssenko, J. Erland, and J. M. Hvam, Phys. Rev. Lett. **76**, 672 (1996).

[6] Z. H. Kafafi, J. R. Lindle, R. G. S. Pong, F. J. Bartoli, L. J. Lingg, and J. Milliken, Chem. Phys. Lett. **188**, 492 (1992).

[7] T. Jakubczyk, V. Delmonte, M. Koperski, K. Nogajewski, C. Faugeras, W. Langbein, M. Potemski, and J. Kasprzak, Nano Lett. **16**, 5333 (2016).

[8] A. J. Fischer, W. Shan, G. H. Park, J. J. Song, D. S. Kim, D. S. Yee, R. Horning, and B. Goldenberg, Phys. Rev. B **56**, 1077 (1997).

[9] T. Aoki, G. Mohs, M. Kuwata-Gonokami, and A. A. Yamaguchi, Phys. Rev. Lett. **82**, 3108 (1999).

[10] M. Z. Maialle, E. A. de Andrada e Silva, and L. J. Sham, Phys. Rev. B **47**, 15776 (1993).

[11] E. Feltin, D. Simeonov, J.-F. Carlin, R. Butté, and N. Grandjean, Appl. Phys. Lett. **90**, 021905 (2007).

[12] F. S. Cheregi, A. Vinattieri, E. Feltin, D. Simeonov, J.-F. Carlin, R. Butté, N. Grandjean, and M. Gurioli, Phys. Rev. B **77**, 125342 (2008).

[13] J. Besbas, A. Gadalla, M. Gallart, O. Crégut, B. Hönerlage, P. Gilliot, E. Feltin, J. F. Carlin, R. Butté, and N. Grandjean, Phys. Rev. B **82**, 195302 (2010).

[14] J. Erland and I. Balslev, Phys. Rev. A **48**, R1765 (1993).

[15] See Supplemental Material at http://link.aps.org/supplemental/10.1103/PhysRevB.96.041303 for the determination of the inhomogeneous broadening of quantum well A and B excitons by linear reflectivity measurements.

[16] A. Honold, L. Schultheis, J. Kuhl, and C. W. Tu, Phys. Rev. B **40**, 6442(R) (1989).

[17] D.-S. Kim, J. Shah, J. E. Cunningham, T. C. Damen, W. Schäfer, M. Hartmann, and S. Schmitt-Rink, Phys. Rev. Lett. **68**, 1006 (1992).

[18] L. C. Andreani and F. Bassani, Phys. Rev. B **41**, 7536 (1990).

[19] M. Julier, J. Campo, B. Gil, J. P. Lascaray, and S. Nakamura, Phys. Rev. B **57**, R6791 (1998).

[20] E. Blackwood, M. J. Snelling, R. T. Harley, S. R. Andrews, and C. T. B. Foxon, Phys. Rev. B **50**, 14246 (1994).

[21] P. Ramvall, S. Tanaka, S. Nomura, P. Riblet, and Y. Aoyagi, Appl. Phys. Lett. **73**, 1104 (1998).

[22] F. Stokker-Cheregi, A. Vinattieri, E. Feltin, D. Simeonov, J. Levrat, J.-F. Carlin, R. Butté, N. Grandjean, and M. Gurioli, Appl. Phys. Lett. **93**, 152105 (2008).